ORGANIC PROCESS RESEARCH & DEVELOPMENT
OPR&D
Article
Cite This: Org. Process Res. Dev. XXXX, XXX, XXX–XXX
pubs.acs.org/OPRD

One-Step Synthesis of 2-Fluoroadenine Using Hydrogen Fluoride Pyridine in a Continuous Flow Operation

Nastaran Salehi Marzijarani,*[,†,§] David R. Snead,[†,§] Jonathan P. McMullen,[†] François Lévesque,[†] Mark Weisel,[†] Richard J. Varsolona,[†] Yu-hong Lam,[‡] Zhijian Liu,[†] and John R. Naber*[,†]

[†]Process Research & Development, MRL, Merck & Co. Inc., P.O. Box 2000, Rahway, New Jersey 07065, United States
[‡]Modeling and Informatics, Merck & Co. Inc., P.O. Box 2000, Rahway, New Jersey 07065, United States

Supporting Information

ABSTRACT: We report the development of a one-pot synthesis of 2-fluoroadenine from an inexpensive 2,6-diaminopurine starting material using diazonium chemistry in a continuous fashion. Given the sensitivity of this transformation to temperature, we conducted critical experiments to study the exothermicity of the reaction and the heat removal, which were critical for the development of the process. Our goal was to improve the yield and purity of this pharmaceutical intermediate (2-fluoroadenine) and develop a more robust process.

KEYWORDS: *flow chemistry, continuous, exothermic, fluorination, diazonium, nitrite, temperature-sensitive*

INTRODUCTION

The selective introduction of a fluorine atom in biologically active molecules, especially in nucleosides for interrupting cancer cell or viral replication, has received significant attention in recent years.[1] The main driver for the incorporation of fluorine is the similarity in size of fluorine and hydrogen atoms and the higher biological and chemical stability of organofluorine compounds.[1a,2] The interest in 2-fluoroadenine nucleosides is increasing, with cytotoxic 2-fluoroadenosine and modified sugar analogues demonstrating resistance toward deamination by the catabolic enzyme adenosine deaminase and thus longer lifetimes in vivo.[3] Many efficient synthetic methodologies have been reported for the formation of sp^2 C−F bonds, though many require a directing group, such as a weak amide, or have a limited substrate scope.[4] Many of the more efficient approaches have not been applied to the synthesis of 2-fluoroadenine because of the high polarity and lack of solubility of this compound in most organic solvents. The existing methods are lengthy, require protecting group manipulations, or employ expensive starting materials. They also suffer from low overall yield or require the use of chromatographic purification because of low selectivity.[5] The most commonly reported approach for the synthesis of 2-fluoroadenine is the nucleophilic fluorination of aryl diazonium salts in tetrafluoroboric acid (the Balz−Schiemann reaction).[6] However, the reactivity of this polar compound necessitates the use of aqueous conditions because of its low solubility in organic solvents, and the fluorination step has been shown to be very challenging under these conditions with low yields, mainly because of competition between fluorine addition and formation of the appropriate HO-purine as a byproduct.[7] To avoid the use of water, HF/Pyridine has been shown to be an effective fluorinating reagent.[8] Moderate yields reported for the synthesis of 2-fluoroadenine and scale-up challenges we encountered with the use of HF/Pyridine in batch mode encouraged us to explore the use of continuous flow processing for this transformation.[8c]

Continuous flow systems are gaining popularity for the synthesis of pharmaceutical ingredients and intermediates.[9] Importantly, improved control of reaction parameters such as heat and mass transfer, mixing, and residence time are some of the benefits arising from continuous flow compared with related batch processes, and these advantages can often lead to improved process safety and robustness.[10] Herein we present the synthesis of 2-fluoroadenine in continuous flow, where a thorough understanding of heat transfer and several rounds of optimization led to an efficient synthesis in high yield with high selectivity.

RESULTS AND DISCUSSION

Part 1: Reaction Optimization and Understanding of Batch Operation. The initial exploration of the reaction in batch mode focused on screening of temperature, nitrite sources/equivalents, solvents, acid sources, and fluorine sources. The starting material, 2,6-diaminopurine (**1a**), is sparingly soluble (less than 2 mg/mL) in most organic solvents, with a maximum room-temperature solubility of only 17 mg/mL in *N*,*N*-dimethylacetamide (DMAc). Most of the conditions screened led to low reactivity. The highest conversions were found in aqueous environments. However, these conditions resulted in low yields due to trapping of the diazonium salt intermediate with water (see Table S1 in the Supporting Information (SI)). After several rounds of optimization, we found that the highest yields and conversions could be achieved using *tert*-butyl nitrite (*t*BuONO) in neat hydrogen fluoride pyridine solution (HF/Pyridine). Further

Special Issue: Honoring 25 Years of the Buchwald-Hartwig Amination

Received: April 26, 2019

DOI: 10.1021/acs.oprd.9b00178
Org. Process Res. Dev. XXXX, XXX, XXX–XXX

Table 1. Optimization of the Synthesis of 2-Fluoroadenine (2a) in Batch Operation

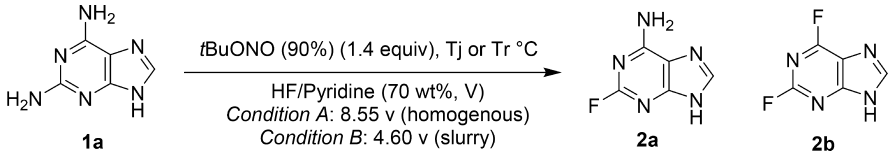

entry	condition	scale (g)	T_j or T_r[a]	presssure (psi)	addition time (min)	conv. (%)	2a (%)	2b (%)	yield (%)
1	A	0.8	T_j = 0 °C	–	8	99.6	88.5	8.8	–
2	A	4.0	T_j = 0 °C	–	8	78.1	62.1	0.8	–
3[b]	A	4.0	T_r = 0 °C	40–350	45	97.7	90.0	3.5	74
4[b]	A	4.0	T_r = 0 °C	40–45	45	96.7	85.5	3.7	68
5[b]	A	4.0	T_r = 0 °C	0.5	45	97.1	88.2	4.0	69
6[b,c]	B	10.0	T_r = −5 °C	0.5	25	99.2	82.4	13.8	72

[a] T_j is the jacket temperature, and T_r is the temperature inside the reaction vessel. A discussion of safety issues associated with handling HF/Pyridine and how to minimize them is provided in the Supporting Information. [b] A Multimax/Easymax system was used for T_r control. [c] 1.1 equiv of nitrite was used after rounds of optimization.

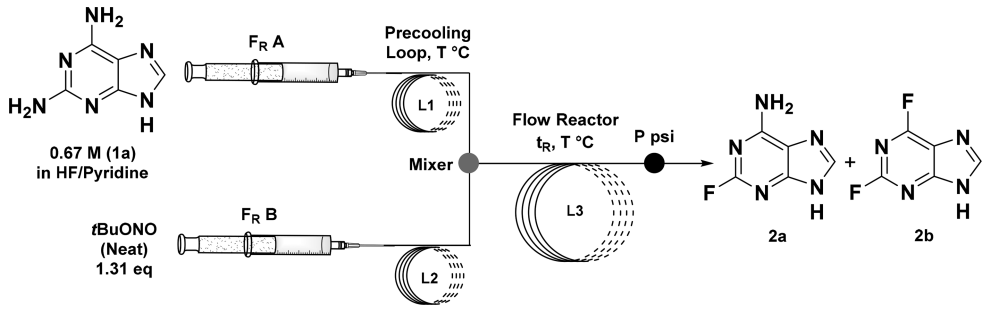

Figure 1. Lab-scale flow reactor setup.

optimization led to the reaction conditions shown in Table 1 (see Table S2 for more details). Selectivity for the reaction of the amine at the 2-position in preference to the 6-position was observed; however, overfluorination was observed in some cases. In our initial optimization, we observed variability in conversion when the reaction scale was increased in batch (Table 1, entries 1 and 2). The conversion dropped significantly, with 5–12% of **1a** remaining unreacted with the same nitrite addition time (8 min) when the scale was changed from 800 mg to 4 g. This was explained by the temperature that was measured inside the reaction vessel, which reached 35 °C. We discovered that both the conversion and the percentage of overfluorinated impurity **2b** can be impacted significantly by the temperature and the rate of nitrite addition. Although the overfluorinated impurity **2b** could be easily removed during isolation (precipitation of the reaction stream with EtOAc), the reaction yield was directly impacted by higher amounts of this impurity. Achieving a purity of more than 98% was essential for our process, and our goal was to develop a robust crystallization and to avoid chromatographic purification. We were successful in this goal and discovered a crystallization method that was optimized to improve the purity of 2-fluoroadenine to more than 98% (see the SI). It was found that complete rejection of starting material **1a** during this crystallization was difficult at conversions lower than 95%, and residual 2,6-diaminopurine was the main impurity after our crystallization process. As a result, the reaction was optimized to target complete conversion while simultaneously minimizing impurity **2b**, as shown in Table 1, entries 3–6. We found that the headspace pressure did not affect the conversion, but we observed an increase in overfluorinated byproduct when the pressure was reduced from 350 to 50 psi (entries 3–5).

The high sensitivity of the reaction to temperature was explained by the short half-life of *t*BuONO in HF/Pyridine at higher temperatures. Subsequent investigation led to the realization that the reaction is rapid, highly exothermic, and sensitive to temperature rise. The active species to form diazonium salts, NOF, which was observed in situ by Raman spectroscopy at ~2340 cm^{-1}, was very unstable above ambient temperatures and found to decompose within 1 h of incubation (see the SI).[11] Therefore, the longer incubation of *t*BuONO in HF/Pyridine (liquid or vapor in the headspace) resulted in higher levels of this decomposition and lower conversion. This hypothesis was confirmed by a premixing experiment in both temperature-controlled and temperature-uncontrolled experiments (Figure S4 in the SI), in which the degradation of *t*BuONO was faster at higher temperature. The lack of robustness toward minor changes in the process led us to explore the use of a continuous flow system to ensure better heat transfer and ultimately achieve a more robust process.

Part 2: Reaction Optimization in Flow Operation.[12] The study of the reaction in continuous flow was performed in the reactor setup shown in Figure 1. A solution of **1a** in HF/Pyridine was prepared and loaded into a stainless steel (SS) syringe, and neat *t*BuONO was loaded into a second SS syringe. Solutions were pumped with a syringe pump at a total flow rate of 0.2 mL/min. Perfluoroalkoxyalkane (PFA) precooling loops (0.063″ o.d., 0.03″ i.d.), constructed to give 1 min of precooling residence time (t_R), were made for each stream and joined by a PEEK tee mixer (0.02″ i.d.). The length of the PFA flow reactor loop (0.063″ o.d., 0.03″ i.d.) was varied to adjust the t_R for kinetic analysis. Pressure was

DOI: 10.1021/acs.oprd.9b00178
Org. Process Res. Dev. XXXX, XXX, XXX−XXX

controlled with a 100−250 psi back-pressure regulator (BPR). The precooling loops, reactor, and BPR were cooled to 0 °C in an ice bath.

The initial results with a flow rate of 0.2 mL/min in a plug flow reactor were encouraging, giving slight improvements to the product distribution (Table 2). More in-depth examination of the amount of *t*BuONO, the residence time, and the temperature demonstrated an ability to tune the conversion by varying the amount of oxidant. A higher amount of oxidant (1.47 equiv, entry 1) resulted in overfluorination (15.7%) and a loss in yield. Reducing the amount of *t*BuONO to 1.16 equiv led to low conversion (94%, entry 2), and extending the residence time for longer aging did not improve the conversion. Finally, we found the optimal amount of *t*BuONO to be 1.31 equiv (entries 3−5). The appropriate t_R was determined in a semicontinuous fashion where the flow reactor effluent was collected and analyzed for reaction conversion at various time points with agitation at 0 °C. We discovered that the reaction approaches 80% conversion very quickly, within 1 min upon mixing, but that the reaction requires 20 min to achieve the targeted conversion. Repeating the flow experiment with 1.31 equiv of *t*BuONO at 0 °C with a residence time of 20 min provided 97.1% conversion with a high selectivity of 93.9% (Table 2, entry 5). More details on high-throughput screening of different variables are discussed in the SI. Substituting PFA tubing for stainless steel led to improved temperature control and slight improvements in the product profile (see the SI). However, for simplicity of operation, transparency, and monitoring inside the flow reactors, PFA tubing was utilized for all the optimizations and scale-ups in the next sections.

Table 2. Initial Optimization of the Flow Process (0.2 mL/min)[a]

entry	equiv of *t*BuONO	L3 t_R (min)	*T* (°C)	pressure (psi)	conv. (%)	**2a** (%)	**2b** (%)
1	1.47	5.0	0	100	97.9	77.9	15.7
2	1.16	20.0	0	100	94.0	90.0	2.7
3	1.31	7.5	0	100	96.6	91.9	0.5
4	1.31	7.5	0	250	96.9	86.5	6.8
5	**1.31**	**20.0**	**0**	**100**	**97.1**	**93.9**	**0.7**
6	1.35	20.0	0	100	97.8	91.4	4.2

[a]Flow optimizations on a small scale (0.2 mL/min). A residence time (t_R) of 1 min was used for L1 and L2 for all entries at 0 °C (all used a 0.02″ i.d. tee mixer).

The reaction was then scaled up from 0.2 to 2 mL/min with the best conditions from the initial optimization. While the temperature, pressure, amount of *t*BuONO, and residence time were held constant at 0 °C, 100 psi, 1.31 equiv, and 20 min, respectively, the tubing size was changed from 0.03″ i.d. to 0.063″ i.d.. This led to higher levels of overfluorinated impurity **2b** and a drop in 2-fluoroadenine (**2a**) from 93.9% to 86.9% (Table 3, entries 2 and 3). Examination of the system revealed that the result was likely caused by an internal temperature rise of the reaction solution due to poor heat transfer in the wider-bore tubing. This hypothesis was tested at low flow rates by increasing the reactor temperature from 0 °C to ambient temperature while maintaining the precooling loop temperatures at 0 °C (entries 1 and 2), which showed the same trend with lower conversion (93.5%) and higher formation of overfluorinated impurity **2b** (8.9%). Next, we reduced the temperature of reactor L3 from 0 to −8 °C at a flow rate of 2 mL/min. Decreasing the L3 temperature helped deliver higher reactivity and selectivity (98.7 conversion, 92.0% **2a**), as shown in Table 3, entries 3−5. Lowering the temperature below −8 °C led to freezing of the *t*BuONO stream and clogging. We realized that the temperature and tube diameter in reactor L3 were more important than the precooling temperatures in L1 and L2. Using narrower tubing (0.032″ i.d.) for the precooling loops L1 and L2 at a flow rate of 2 mL/min did not result in a significant improvement in the selectivity (entry 6). Similarly, when we used −5 °C for the precooling tubes and 0 °C for reactor L3, we did not observe significant improvement (entries 3 and 7). The next step in finding a way to reproduce our best results at the 0.2 mL/min scale (Table 3, entry 2) at higher flow rates was to better understand the root cause of this temperature dependence by measuring the temperature rise inside the tube at different scales.

Part 3: Understanding the Reaction Exotherm and Its Impact on Selectivity in Flow Operation. We first investigated the reaction exotherm and kinetics (see the SI). Because of the hazardous, corrosive nature of the reaction and the lack of equipment compatibility with HF/Pyridine, heats of reaction for mono- and difluorination were estimated using computational chemistry models. Those models indicated that both transformations are exothermic, with the first fluorination (−58.9 kcal/mol) being more exothermic than the second fluorination (−50.1 kcal/mol) by 8.8 kcal/mol. The rate of the first fluorination at position 2 was compared with the rate of the second fluorination at position 6 by stepwise addition of *t*BuONO (see the SI). We observed fluorination only at position 6 when starting from 2-fluoroadenine, which also proceeded at a much lower rate.

The adiabatic temperature rise was estimated to be between 45 and 60 °C, with the reaction reaching ∼80% completion within 1 min. With so much heat released in a short period of time, it was not surprising that overfluorination presented an issue. Additionally, the temperature rise could not only accelerate the decomposition of the active species (nitrosyl

Table 3. Flow Scale-Up Challenges and Importance of Temperature

	T (°C)			PFA tubing i.d.				
entry	L1/L2	L3	flow rate (mL/min)	L1/L2	L3	conv. (%)	**2a** (%)	**2b** (%)
1	0	25	0.2	0.02″	0.02″	93.5	79.9	8.9
2	0	0	0.2	0.02″	0.02″	97.1	93.9	0.7
3	0	0	2.0	0.063″	0.063″	97.7	86.9	7.8
4	0	−5	2.0	0.063″	0.063″	98.1	89.8	6.5
5	0	−8	2.0	0.063″	0.063″	98.7	92.0	5.6
6	0	0	2.0	0.032″	0.063″	97.9	89.6	6.5
7	−5	0	2.0	0.063″	0.063″	97.8	88.5	6.9

DOI: 10.1021/acs.oprd.9b00178
Org. Process Res. Dev. XXXX, XXX, XXX−XXX

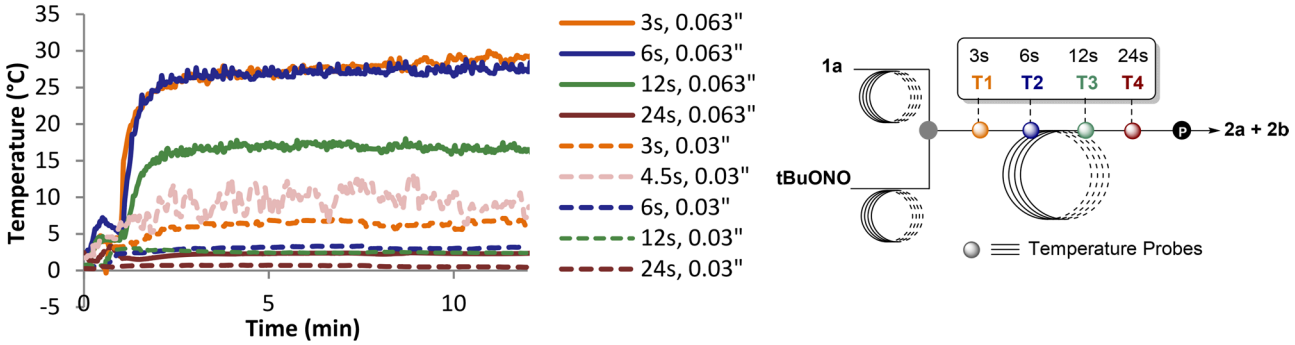

Figure 2. Reaction temperature as a function of tube diameter and t_R at a flow rate of 2 mL/min. Conditions: 1.31 equiv of *t*BuONO, **1a** (0.67 M in HF/Pyridine), T_j = 0 °C.

fluoride), affecting the conversion and selectivity, but also generate more safety issues with handling of the diazonium intermediate. Diazonium moieties are known to be highly energetic, and detonations can be readily initiated by heat and shock, especially with solid-state diazoniums. Therefore, diazonium species often are not isolated but instead are directly used in further reactions. Buildup of diazonium salt was not a concern in our system, in which desired product was formed with no isolation of the diazonium intermediate, because of the high electrophilicity and rapid fluorination. Additionally, several reports have shown that the continuous flow can be used as a tool to mitigate safety concerns related to diazonium salts.[6b,13] We utilized flow chemistry to continuously prepare our transient diazonium species and directly couple it into a subsequent consuming step with an enhanced safety profile. Next, we performed various experiments to find the best conditions for obtaining the best heat control.

While the large exotherm suggests that slow addition of the nitrite may be advantageous, the short lifetime of the active species complicates this process, and we observed decreased conversion in our semibatch process. Subsurface feedings were not explored, as it was expected that backflow into the feed tube may pose a significant challenge. During our scale-up with batch operations, we did observe low conversion and lack of robustness when the *t*BuONO feeding tube was located above the surface. This was mainly due to decomposition of the oxidant at the tip of the dosing tube at longer dosing times (along with solidification and freezing of the oxidant).

To obtain a reaction temperature profile for the 2 mL/min scale reaction (Table 3), thermocouples were inserted into the reactor tubing to measure the temperatures at various positions (T1 to T4 in Figure 2) in the reactor loop (L3). Our goal was to understand the temperature rise shortly after mixing (T1, 3 s after mixing) and as the reaction stream continued through L3 (T2–T4, t_R = 6, 12, and 24 s, respectively). The temperature readings at these four locations were measured for two experiments, one using 0.03″ i.d. tubing and another using wider tubing (0.063″ i.d.). The difference in temperature between the two configurations was striking. In the first system with thinner tubing (0.03″ i.d.), the temperatures were never observed to rise above 12 °C (3–24 s residence time). Within 3–5 s of mixing (T1), the reaction temperature rose to 10–12 °C and then quickly decreased to 4–5 °C prior to reaching T2 (t_R = 6 s), and then at T4 (t_R = 24 s) the reaction temperature was close to zero. Next, we repeated the same experiment for the second system with a larger tubing diameter (0.063″ i.d.) and measured the temperatures at all four locations (T1–T4). When the radial dimension was increased to 0.063″, the maximum temperature observed was 27 °C at T1 and T2 (t_R = 3–6 s). Not only was the temperature higher, it also stayed above 0 °C for a longer period of time (15 °C at T4), which led to decomposition of the nitrite source and eventually to lower conversions and lower selectivity.

Table 4 shows more details on the relationship between the maximum temperature rise, tube diameter, and tube wall thickness. Interestingly, for our system the use of tubing with an even narrower channel width (0.01″ i.d., 0.026″ wall thickness) resulted in the lowest rise in temperature (1.8 °C), but the product distribution did not improve relative to the baseline conditions (0.032″ i.d. tubing). This suggests that the fluorination is tolerant toward some degree of warming. Our results show a strong dependence of the maximum temperature on the tube diameter. It is also well-known that for exothermic reactions, the rate of heat transfer is highly dependent on three factors: (1) the rate of heat generation by the reaction, (2) the rate of heat removal to the reactor wall through convection or conduction, and (3) the rate of heat removal from the reactor wall to the surroundings. Our results suggested that heat transfer through the solution was the limiting factor, not heat transfer across the tube wall. By going to larger-diameter tubing, the surface area to volume ratio decreases, so a longer time for diffusion is required and the heat transfer is less effective. Smaller-diameter tubing increases the surface area to volume ratio and thus increases heat transfer. The larger the surface area to volume ratio, the smaller is the temperature rise at a flow rate of 2 mL/min.

Table 4. Maximum Temperature Rise as a Function of Tube Diameter

entry	tube diameter	wall thickness	surface area to volume ratio	max *T* (°C)
1	0.063″	0.031″	9.9	27.0
2	0.032″	0.016″	21.0	9.5
3	0.010″	0.026″	62.0	1.8

Several strategies were explored to improve the reaction upon scale-up, including lowering the temperature of the cooling bath, applying a mix-then-reside approach, and/or multiport addition of nitrite (Table 5). It was found that when the temperature of the cooling medium was reduced to −8 °C, the results were similar to those observed in thinner tubing. This further confirmed that the internal temperature was the critical variable impacting the ability to scale, as already demonstrated in Table 3. Running at lower temperature provided a solution at this scale; however, the strategy might

DOI: 10.1021/acs.oprd.9b00178
Org. Process Res. Dev. XXXX, XXX, XXX−XXX

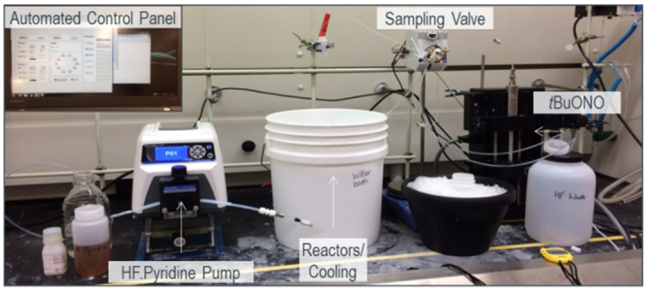

entry	flow-Rate	**1a** (%)	**2a** (%)	**2b** (%)
1	10 mL/min	1.31	91.47	3.09
2	20 mL/min	1.59	91.58	3.08

Figure 3. Successful scale-up to a flow rate of 20 mL/min on an automated platform with multiport addition of *t*BuONO.

Table 5. Higher Flow Rates with Various Tubing Diameters and/or Numbers of Oxidant Inlets

entry	flow rate (mL/min)	no. of nitrite inlets	PFA tubing i.d.	conv. (%)	**2a** (%)	**2b** (%)
1	2.0	1	0.063″	97.7	86.9	7.8
2	2.0	1	0.032″	98.8	91.1	6.3
3	2.0	1	0.032″/0.063″	98.2	90.6	2.9
4	2.0	2	0.032″	98.5	91.7	5.4
5	10.0	1	0.032″/0.09″	97.3	87.9	5.7
6	10.0	4	0.063″	99.0	90.8	5.8

not be applicable to further increases in the radial dimension, especially when scaling to significantly larger diameter tubing with thicker walls. Another challenge with this approach is that lower temperature (below 0 °C) increases the risk of *t*BuONO freezing and clogging.

Next, we looked into a mix-then-reside approach to improve the cooling process in the tubular reactor. We examined this idea at a 2 mL/min scale by having a first reactor coil with a narrow diameter and stainless steel construction for improved heat transfer and a second coil with a wider bore for increased residence time to allow for full reaction completion (Table 5, entries 3 and 5). Mix-then-reside was successfully employed by constructing a first reactor segment of 1/16″ stainless steel tubing (4 mL) that then flowed into a 1/8″ PFA reactor (16 mL). This provided efficient heat transfer in the critical early stages of the reaction (highest temperature rise) and a greater volume for the reaction to reach completion in a larger diameter tubing to reduce pressure drop. While this approach was successful at both the 2 and 10 mL/min scales, there were concerns about the ability to scale-up this system to much higher flow rates.

A more general approach might result from splitting the addition of *t*BuONO into multiple portions to decrease the energy released into the reaction stream at one time, and this was tested next (Table 5). This strategy proved to be successful for reactions run at both 2 and 10 mL/min (Table 5, entries 4 and 6). A multiport system was constructed with four nitrite streams using 0.063″ tubing for the reactor, and experiments at 10 mL/min resulted in conversion and selectivity identical to those obtained in thin tubing at 0.2 mL/min (99.0% conversion, 90.8% selectivity). This approach is viewed as scalable, where the number of sequential *t*BuONO addition points is dependent upon the heat removal rates at the desired reactor scale.

Further demonstrating the applicability of this concept, the flow rate of the reaction was doubled to 20 mL/min, and results identical to those obtained at 10 mL/min were obtained. For improved safety, the reaction was performed on an automated platform[14] to enable hands-free operation in a fully enclosed fume hood at higher reaction volumes (Figure 3). To this end, the syringe pump, peristaltic pump, and sampling valve could all be controlled by computer. In this way, the current reactor setup was deemed to have sufficient throughput capability to meet a significant portion of potential commercial demand as part of a small-volume program. The overall process scheme is shown in Scheme 1. With the current reaction setup and a flow rate of 20 mL/min, 120 g of crude 2-fluoroadenine (**2a**) can be synthesized in 1 h. Next, the collected stream mainly containing **2a** and HF/Pyridine was poured into ethyl acetate (25 volumes). The desired product (crude) was precipitated with very small mother liquor loss, and great rejection of overfluorinated impurity **2b** and HF/Pyridine reagent was observed. The crude solid was dissolved in water and acetonitrile for a pH-swing crystallization using sodium hydroxide and acetic acid in order to upgrade the purity of **2a** to more than 98% (for details, see the SI).

CONCLUSION

We have reported the synthesis of 2-fluoroadenine from commercially available and inexpensive 2,6-diaminopurine through diazonium chemistry without prefunctionalization in one step. We found that this reaction is rapid and exothermic and that it is the root cause of the low conversion and selectivity when the temperature is not well-controlled. By comparison of results obtained in batch to those obtained in flow at different scales, it was found that it was easier to control

Scheme 1. Overall Process Scheme

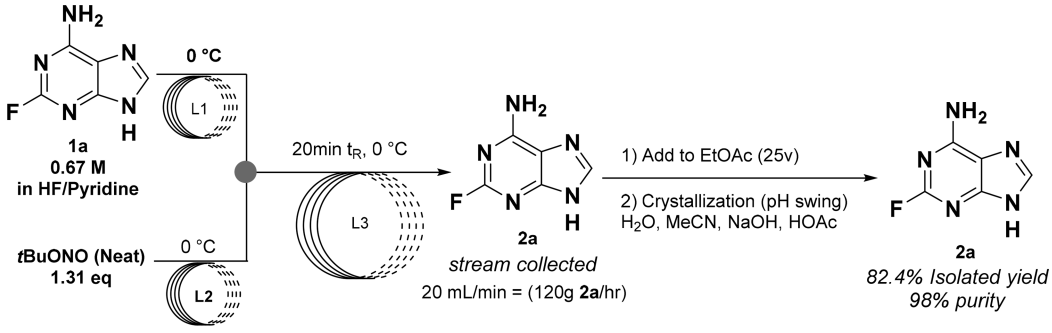

DOI: 10.1021/acs.oprd.9b00178
Org. Process Res. Dev. XXXX, XXX, XXX−XXX

the heat transfer with the continuous operation. Process improvement was established by understanding the impact of temperature, heat transfer, and residence time for this highly exothermic and temperature-sensitive reaction using a tubular reactor. Consistent and scalable results were delivered while using less *t*BuONO (1.31 equiv in comparison with 1.40 equiv in batch), and improvements observed in the **2a** selectivity translated to yields that were approximately 10% higher than the batch analogues (82.4% isolated yield). The high selectivity for 2-fluoroadenine achieved from this process helped us deliver material that was >98% pure with a single crystallization and avoided lengthy chromatographic purification. We developed a safer process to synthesize an important intermediate for a low-dose pharmaceutical drug by both controlling the heat formation in the reaction and using an automated platform to avoid operator contact with the reaction stream. This platform not only allows for automated and continuous operation but also enables the chemists to execute more potentially hazardous transformations in a safe and reliable fashion. We hope that this publication will serve as a guide to some considerations that are important when designing a continuous process for highly exothermic reactions toward manufacturing route development.

■ ASSOCIATED CONTENT

Supporting Information

The Supporting Information is available free of charge on the ACS Publications website at DOI: 10.1021/acs.oprd.9b00178.

Remaining experimental procedures and a discussion of the equipment used (PDF)

■ AUTHOR INFORMATION

Corresponding Authors

*E-mail: nastaran.salehi.marzijarani@merck.com.
*E-mail: john.naber@merck.com.

ORCID

Nastaran Salehi Marzijarani: 0000-0001-8940-4674
Jonathan P. McMullen: 0000-0001-5969-2396
François Lévesque: 0000-0001-9529-4993
Zhijian Liu: 0000-0002-5750-9890
John R. Naber: 0000-0002-4390-3467

Author Contributions

§N.S.M. and D.R.S. contributed equally.

Notes

The authors declare no competing financial interest.

■ ACKNOWLEDGMENTS

We acknowledge Simon Hamilton and David Waterhouse for their analytical support, George Zhou and Zachary Dance for their help with Raman spectroscopy, Ryan Cohen for NMR analysis, Thomas Vickery for DSC measurements, Shane Grosser for help with automation, and Benjamin Sherry for all the support throughout this project.

■ REFERENCES

(1) (a) Liu, P.; Sharon, A.; Chu, C. K. Fluorinated nucleosides: Synthesis and biological implication. *J. Fluorine Chem.* **2008**, *129* (9), 743−766. (b) Wójtowicz-Rajchel, H. Synthesis and applications of fluorinated nucleoside analogues. *J. Fluorine Chem.* **2012**, *143*, 11−48.

(2) Wilkinson, J. A. Recent advances in the selective formation of the carbon-fluorine bond. *Chem. Rev.* **1992**, *92* (4), 505−519.

(3) (a) Robins, M. J.; Uznański, B. Nucleic acid related compounds. 34. Non-aqueous diazotization with tert-butyl nitrite. Introduction of fluorine, chlorine, and bromine at C-2 of purine nucleosides. *Can. J. Chem.* **1981**, *59* (17), 2608−2611. (b) Baer, H.-P.; Drummond, G. I.; Duncan, E. L. Formation and Deamination of Adenosine by Cardiac Muscle Enzymes. *Mol. Pharmacol.* **1966**, *2* (1), 67−76.

(4) (a) Yamamoto, K.; Li, J.; Garber, J. A. O.; Rolfes, J. D.; Boursalian, G. B.; Borghs, J. C.; Genicot, C.; Jacq, J.; van Gastel, M.; Neese, F.; Ritter, T. Palladium-catalysed electrophilic aromatic C−H fluorination. *Nature* **2018**, *554*, 511. (b) Campbell, M. G.; Ritter, T. Modern Carbon−Fluorine Bond Forming Reactions for Aryl Fluoride Synthesis. *Chem. Rev.* **2015**, *115* (2), 612−633. (c) Zhang, Y.; Wen, C.; Li, J. C5-Regioselective C−H fluorination of 8-aminoquinoline amides and sulfonamides with Selectfluor under metal-free conditions. *Org. Biomol. Chem.* **2018**, *16* (11), 1912−1920. (d) Lin, A.; Huehls, C. B.; Yang, J. Recent advances in C−H fluorination. *Org. Chem. Front.* **2014**, *1* (4), 434−438. (e) Grushin, V. V. The Organometallic Fluorine Chemistry of Palladium and Rhodium: Studies toward Aromatic Fluorination. *Acc. Chem. Res.* **2010**, *43* (1), 160−171. (f) Ning, X.-Q.; Lou, S.-J.; Mao, Y.-J.; Xu, Z.-Y.; Xu, D.-Q. Nitrate-promoted Selective C−H Fluorination of Benzamides and Benzeneacetamides. *Org. Lett.* **2018**, *20* (8), 2445−2448.

(5) (a) Wang, J.-j.; Sun, X.-y.; Chen, J.-b. New Method for the Synthesis of 2-Fluoroadenine. *Chin. J. Synth. Chem.* **2007**, *15* (4), 506−507. (b) Giner-Sorolla, A.; Burchenal, J. H. Substituted hydroxylaminopurines and related derivatives. *J. Med. Chem.* **1971**, *14* (9), 816−819.

(6) (a) Mohy El Dine, T.; Sadek, O.; Gras, E.; Perrin, D. M. Expanding the Balz−Schiemann Reaction: Organotrifluoroborates Serve as Competent Sources of Fluoride Ion for Fluoro-Dediazoniation. *Chem. - Eur. J.* **2018**, *24* (56), 14933−14937. (b) Park, N. H.; Senter, T. J.; Buchwald, S. L. Rapid Synthesis of Aryl Fluorides in Continuous Flow through the Balz−Schiemann Reaction. *Angew. Chem., Int. Ed.* **2016**, *55* (39), 11907−11911.

(7) Montgomery, J. A.; Hewson, K. Synthesis of Potential Anticancer Agents. XX. 2-Fluoropurines2. *J. Am. Chem. Soc.* **1960**, *82* (2), 463−468.

(8) (a) Eaton, C. N.; Denny, G. H. Synthesis of 2-fluoroadenine. *J. Org. Chem.* **1969**, *34* (3), 747−748. (b) Olah, G. A.; Welch, J. T.; Vankar, Y. D.; Nojima, M.; Kerekes, I.; Olah, J. A. Synthetic methods and reactions. 63. Pyridinium poly(hydrogen fluoride) (30% pyridine-70% hydrogen fluoride): a convenient reagent for organic fluorination reactions. *J. Org. Chem.* **1979**, *44* (22), 3872−3881. (c) Saischek, G. Process for the preparation of 2-fluoroadenine. US 2009/0163713 A1, 2009.

(9) (a) McMullen, J. P.; Marton, C. H.; Sherry, B. D.; Spencer, G.; Kukura, J.; Eyke, N. S. Development and Scale-Up of a Continuous Reaction for Production of an Active Pharmaceutical Ingredient Intermediate. *Org. Process Res. Dev.* **2018**, *22* (9), 1208−1213. (b) Gutmann, B.; Cantillo, D.; Kappe, C. O. Continuous-Flow Technology—A Tool for the Safe Manufacturing of Active Pharmaceutical Ingredients. *Angew. Chem., Int. Ed.* **2015**, *54* (23), 6688−6728. (c) Baumann, M.; Baxendale, I. R. The synthesis of active pharmaceutical ingredients (APIs) using continuous flow chemistry. *Beilstein J. Org. Chem.* **2015**, *11*, 1194−1219. (d) Cole, K. P.; Groh, J. M.; Johnson, M. D.; Burcham, C. L.; Campbell, B. M.; Diseroad, W. D.; Heller, M. R.; Howell, J. R.; Kallman, N. J.; Koenig, T. M.; May, S. A.; Miller, R. D.; Mitchell, D.; Myers, D. P.; Myers, S. S.; Phillips, J. L.; Polster, C. S.; White, T. D.; Cashman, J.; Hurley, D.; Moylan, R.; Sheehan, P.; Spencer, R. D.; Desmond, K.; Desmond, P.; Gowran, O. Kilogram-scale prexasertib monolactate monohydrate synthesis under continuous-flow CGMP conditions. *Science* **2017**, *356* (6343), 1144.

(10) (a) Plutschack, M. B.; Pieber, B.; Gilmore, K.; Seeberger, P. H. The Hitchhiker's Guide to Flow Chemistry. *Chem. Rev.* **2017**, *117* (18), 11796−11893. (b) Hartman, R. L.; McMullen, J. P.; Jensen, K. F. Deciding Whether To Go with the Flow: Evaluating the Merits of Flow Reactors for Synthesis. *Angew. Chem., Int. Ed.* **2011**, *50* (33), 7502−7519. (c) Yoshida, J.-i.; Takahashi, Y.; Nagaki, A. Flash

DOI: 10.1021/acs.oprd.9b00178
Org. Process Res. Dev. XXXX, XXX, XXX−XXX

chemistry: flow chemistry that cannot be done in batch. *Chem. Commun.* **2013**, *49* (85), 9896−9904. (d) Kockmann, N.; Thenée, P.; Fleischer-Trebes, C.; Laudadio, G.; Noël, T. Safety assessment in development and operation of modular continuous-flow processes. *Reaction Chemistry & Engineering* **2017**, *2* (3), 258−280.

(11) (a) Ruff, O.; Stäuber, K. Über das Nitrosylfluorid (NOF). *Z. Anorg. Chem.* **1905**, *47* (1), 190−202. (b) Flores, A. L.; Darwent, B. d. Photochemical decomposition of nitrosyl fluoride. *J. Phys. Chem.* **1969**, *73* (7), 2203−2208. (c) Addison, C. C.; Lewis, J. The chemistry of the nitrosyl group (NO). *Q. Rev., Chem. Soc.* **1955**, *9* (2), 115−149.

(12) Britton, J.; Jamison, T. F. The assembly and use of continuous flow systems for chemical synthesis. *Nat. Protoc.* **2017**, *12*, 2423.

(13) (a) Deadman, B. J.; Collins, S. G.; Maguire, A. R. Taming Hazardous Chemistry in Flow: The Continuous Processing of Diazo and Diazonium Compounds. *Chem. - Eur. J.* **2015**, *21* (6), 2298−2308. (b) Hu, T.; Baxendale, I. R.; Baumann, M. Exploring Flow Procedures for Diazonium Formation. *Molecules* **2016**, *21* (7), 918.

(14) Ley, S. V.; Fitzpatrick, D. E.; Ingham, R. J.; Myers, R. M. Organic Synthesis: March of the Machines. *Angew. Chem., Int. Ed.* **2015**, *54* (11), 3449−3464.

DOI: 10.1021/acs.oprd.9b00178
Org. Process Res. Dev. XXXX, XXX, XXX−XXX